Thermal effects on the photoelastic coefficient of polymer optical fibers

Acheroy, S.; Merken, Patrick; Ottevaere, Heidi; Geernaert, Thomas; Thienpont, Hugo; Marques, Carlos A.F.; Webb, David J.; Gang-Ding, Peng; Mergo, P.; Berghmans, Francis

Published in:
Opt. Lett.

DOI:
10.1364/OL.41.002517

Publication date:
2016

Optics Letters

Thermal effects on the photoelastic coefficient of polymer optical fibers

Acheroy Sophie,[1,*] Merken Patrick,[1] Ottevaere Heidi,[2] Geernaert Thomas,[2] Thienpont Hugo,[2] Carlos A. F. Marques,[3,4] David J. Webb,[3] Gang-Ding Peng,[5] Pawel Mergo,[6] and Berghmans Francis[2]

[1]Department of Communication, Information, Systems and Sensors, Royal Military Academy, Ave Renaissance 30, 1000 Brussels, Belgium
[2]Vrije Universiteit Brussel (VUB), Department of Applied Physics and Photonics, Brussels Photonics Team (B-PHOT), Pleinlaan 2, B-1050 Brussels, Belgium
[3]Aston Institute of Photonic Technologies, Aston University, Aston Triangle, B4 7ET Birmingham, UK
[4]Instituto de Telecomunicações and University of Aveiro Physics Department & I3N, Campus de Santiago, 3810-193 Aveiro, Portugal
[5]Photonics & Optical Communications, School of Electrical Engineering & Telecommunications, University of New South Wales, Sydney 2052, NSW, Australia
[6]Laboratory of Optical Fibers Technology, Maria Curie-Sklodowska University Sklodowska Sq. 3, 20-031 Lublin, Poland
*Corresponding author: sophie.acheroy@rma.ac.be

Received 23 March 2016; revised 3 May 2016; accepted 3 May 2016; posted 4 May 2016 (Doc. ID 261659); published 23 May 2016

We measure the radial profile of the photoelastic coefficient $C(r)$ in single-mode polymer optical fibers (POFs), and we determine the evolution of $C(r)$ after annealing the fibers at temperatures from 40°C to 80°C. We demonstrate that $C(r)$ in the fibers drawn from a preform without specific thermal pre-treatment changes and converges to values between 1.2 and 1.6×10^{-12} Pa^{-1} following annealing at 80°C. The annealed fibers display a smoothened radial profile of $C(r)$ and a lowered residual birefringence. In contrast, the mean value of $C(r)$ of the fiber drawn from a preform that has been pre-annealed remains constant after our annealing process and is significantly higher, i.e., 4×10^{-12} Pa^{-1}. The annealing process decreases the residual birefringence to a lower extent as well. These measurements indicate the impact of annealing on the thermal stability of the photoelastic coefficient of POFs, which is an essential characteristic in view of developing POF-based thermo-mechanical sensors.

OCIS codes: (060.2400) Fiber properties; (060.2370) Fiber optics sensors; (060.2270) Fiber characterization; (160.5470) Polymers.

http://dx.doi.org/10.1364/OL.41.002517

Polymer optical fibers (POFs) are claimed to offer an interesting alternative to glass optical fibers for sensing applications [1–3]. This essentially stems from the different material properties in terms of physical and chemical characteristics of polymers compared to glass. More specifically and, for example, POFs are more flexible, they can handle larger mechanical strains, they can be processed with organic chemistry techniques, and they can be made biocompatible [4].

Few publications deal with the physical material characteristics and, specifically, the photo-elastic properties of POFs [5–9]. This is in contrast to silica fibers, for which these properties are relatively well documented [10–12]. The knowledge of these characteristics, along with the impact of the fabrication process on their values, is nevertheless important in view of designing and fabricating optical fibers dedicated to sensing applications. In this Letter, we focus on the stress-optic coefficients C_1 and C_2 as material dependent parameters that link the change of the refractive index in the fiber caused by an external load and, more particularly, on the photoelastic constant $C = C_1 - C_2$. Our research has been prompted by [13], which reported that annealing of POFs partially relieves frozen-in stresses induced by the fiber drawing process, and which results in an increase of the sensitivity to stress and strain of the fiber. Additionally, Ref. [14] reports that annealing the fiber reduces the cross-sensitivity of POF-based sensors to both temperature and strain variations.

We have recently developed a method to determine the stress-optic constant C and its radial distribution in the fiber cross section, with the measurement method and algorithm detailed in previous publications [15–17]. The main steps of our method are briefly recalled here for the sake of completeness. We illuminate the optical fiber transversally (along the x-axis) with monochromatic light at 633 nm, polarized at 45° with respect to the fiber axis. The wave vector is perpendicular to the fiber axis taken along the z-axis. Additionally, the fiber is immersed in index matching liquid to avoid refraction phenomena at the fiber-air boundaries. During illumination, we apply a known axial load inducing a normal stress σ_z which is assumed to be constant over the fiber cross section. In its turn, the normal stress induces birefringence in the fiber, which causes a phase shift between the two linear polarized components of the illumination. This is observed as a projected retardance $R(y)$ following propagation through the fiber, where y is the other transversal coordinate. $R(y)$ is related to the normal stress by means of the inverse Abel transform [18]:

$$\sigma_z \times C(r) = -\frac{1}{\pi}\int_r^b \frac{\mathrm{d}R(y)/\mathrm{d}y}{\sqrt{y^2 - r^2}}\,\mathrm{d}y. \quad (1)$$

We can derive the photoelastic constant from Eq. (1). It is the regression coefficient $C(r)$ linking the inverse Abel transform of $R(y)$ and the known axial stress σ_z. r is the radial distance from the center of the fiber, and b is the radius of the fiber.

We measure $R(y)$ using the Sénarmont compensation method. We use a polarizing microscope to achieve a full-field view of the retardance. The algorithm to calculate the inverse Abel transform of $R(y)$ is based on Fourier theory and is extensively described in [15,16], along with the discussion of measurement results on glass optical fibers.

Note that the mean value of C can also be determined. If one assumes that σ_z and C are constant over the fiber cross section, the shape of $R(y)$ can be approximated with a semi-ellipse $E(y)$. The inverse Abel transform of $E(y)$ is constant and depends solely on the semi-short and the semi-long axes of the ellipse. The expression between the axial stress and the retardance then becomes

$$\sigma_z \times C + K_0 = -\frac{1}{2}\frac{a}{b}, \quad (2)$$

where b is the fiber radius, and $a = \max(\mathrm{abs}(R(y)))$; σ_z the axial stress, and K_0 is a constant defined by the inverse Abel transform of the retardance caused by the residual birefringence of the fiber when it is not submitted to an external load. Again, C is the regression coefficient that has to be determined. The elliptical approximation therefore also allows estimation of the residual birefringence in the fiber, assuming that K_0 is constant over the fiber cross section.

Using the technique explained above, we determine $C(r)$ in samples of three similar single-mode step-index polymer optical fibers, labeled Fibers 1 to 3, drawn in the same facility with similar drawing conditions [19–21]. The draw tension for all three fibers was below 1N. The core and cladding dimensions of the fibers are, respectively, 10 μm/110 μm, 10 μm/133 μm, and 12 μm/260 μm. The core of the fibers is composed of poly-ethyl methacrylate and poly-benzyl methacrylate (PEMA/PBzMA) [22], while the cladding is made of poly-methyl methacrylate (PMMA). Variations in drawing conditions can, for example, lead to core/cladding ratio differences resulting from fluctuating fluid dynamic responses of the two polymers (PMMA and PEMA/PBzMA); yet, the largest part of the fiber consists of PMMA considering the small dimensions of the core. Fibers 1 and 2 are fabricated from the same preform, while Fiber 3 was obtained from a second preform. The preforms were obtained following thermal curing of the polymer. For the first preform, the temperature was increased from 45°C to 75°C within four days. The second preform was obtained after heating from 36°C to 88°C within 4.5 days until solidification. The preforms were then heat-drawn into optical fibers at, respectively, 220°C and 225°C.

We first determine both the mean value of C and $C(r)$ for the pristine samples. We then anneal the samples for 8 h at, respectively, 40°C, 60°C, and 80°C; we determine the mean value of C and $C(r)$ following each annealing step. PMMA-based POFs are well known to be sensitive to humidity [23–25]. While we could not control the history in terms of exposure to environmental temperature and humidity changes between their fabrication and arrival in our laboratories, we emphasize that between the annealing steps carried out in our labs, all fiber samples were stored and measured in the same temperature (20°C) and relative humidity (50%) controlled cleanroom and, therefore, in the same environmental conditions. To ensure that the fibers were uniform along their lengths, we have carried out measurements on several fiber portions taken from a single fiber length. We obtained similar results in terms of value of C (not shown here for the sake of conciseness), which confirms the axial uniformity of the measured fibers.

Figure 1 illustrates the results obtained for Fibers 1 and 2. Similar graphs are obtained for Fiber 3. The constant K_0 of the fiber clearly decreases with increasing annealing temperatures, indicating the decrease of the residual birefringence and, hence, of the residual stress in these samples. K_0 in the samples annealed at 80°C is 36% lower for Fibers 1 and 2, and 17% lower for Fiber 3 compared to the pristine samples.

The mean value of the stress-optic coefficient tends to reach comparable values between 1.2×10^{-12} Pa^{-1} to 1.6×10^{-12} Pa^{-1} for the three fibers. Table 1 summarizes the values of C and the constant K_0 we measured on the three fibers for increasing annealing temperature.

The radial profile $C(r)$ of the pristine fiber samples and those of the samples annealed at 40°C and 60°C are comparable. After annealing at 80°C, however, the effect of the higher temperature is clearly visible. Therefore, and for the sake of clarity, we only compare the $C(r)$ profiles before annealing and after annealing at 80°C in Fig. 2. This annealing process increases the value of the mean stress-optic constant. The variance of the measurements of Fiber 2 without annealing is slightly higher than that of Fiber 1. This has a direct impact on the calculation and result of the inverse Abel transform of the

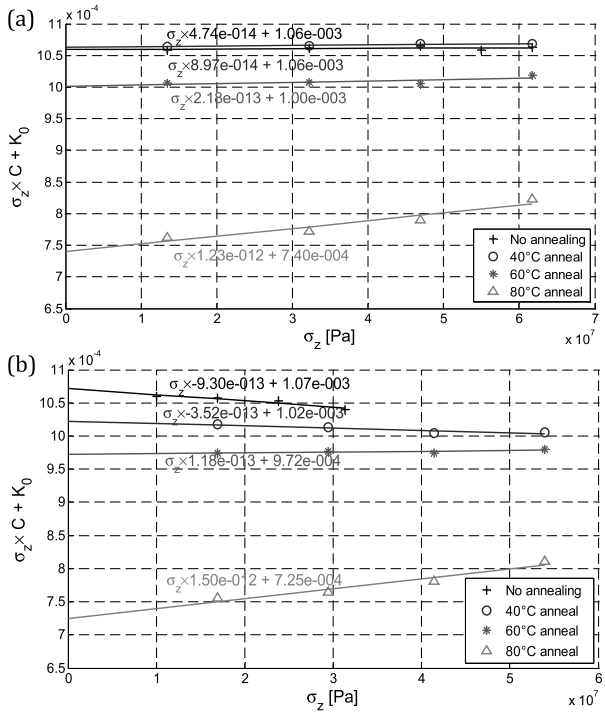

Fig. 1. $\sigma_z \times C + K_0$ as a function of the axial stress measured on a sample of (a) Fiber 1 and (b) Fiber 2. The regression coefficient is the mean photoelastic constant C. The values of C and the extrapolated values of the residual stress are indicated in the graph along the respective linear fits.

Table 1. Measured Stress-Optic Coefficient and K_0 for Fibers for Different Annealing Temperatures

		Fiber 1	Fiber 2	Fiber 3	Fiber 4	Fiber 5
Diameter [µm]	**Temperature**	**110**	**133**	**260**	**110**	**210**
Draw tension D_T		<<1 N	<<1 N	<<1 N	[a]	$0.5<D_T<1$ N
Draw ratio [mm]		16/0.11	16/0.133	16/0.26	[a]	11/0.21
$C[\times 10^{-12}$ Pa$^{-1}]$	No	0.047	−0.93	0.504	−0.15	3.85
	40°C	0.089	−0.35	0.75	−0.124	4.08
	60°C	0.218	0.118	1.06	−0.099	3.83
	80°C	1.23	1.50	1.57	1.54	3.94
$K_0[\times 10^{-4}]$	No	11	11	5.9	10	2.3
	40°C	11	10	5.9	9	2.3
	60°C	10	10	5.6	8	2.3
	80°C	7.4	7.2	4.8	6	2.1

[a]The draw tension and draw ratio for Fiber 4 have not been communicated by the manufacturer.

retardance. Our results clearly show the effect of annealing the POFs at a higher temperature. The variance decreases in both fibers, which explains a smoother and more constant $C(r)$ profile throughout the fiber cross section. Note that the overshoot at $r = 0$, i.e., in the center of the fiber, stems from a numerical artifact of the inverse Abel transform. The height of the overshoot depends on the amount of Fourier coefficients considered in the expansion of the inverse Abel transform, as we explained in detail in [15], and cannot be related to an actual property of the optical fiber.

To substantiate our findings, we repeated the same measurements on two other types of single-mode polymer fibers (Fibers 4 and 5). Fiber 4 has a PMMA core doped with 5% polystyrene and a cladding composed of pure PMMA [26,27]. Fiber 5 also has a PMMA cladding and a core composed of PMMA doped with 2,4,6-trichlorophenil methacrylate. The preform of Fiber 5 was annealed for two weeks at 80°C before the fiber was heat-drawn at 290°C with a draw tension below 1N. The core/cladding dimensions of these two fibers are, respectively, 9 µm/110 µm and 4 µm/210 µm.

Figure 3 shows the mean value of C. The impact of annealing on Fiber 4 is comparable to that on Fibers 1 to 3. K_0 decreases significantly, while the mean value of C increases from -2.63×10^{-13} Pa^{-1} to 1.60×10^{-12} Pa^{-1}. In Fiber 5, for which the preform has been annealed prior to drawing, the decrease of K_0 is less pronounced (7.7%), but the mean value of C also remains almost constant. Figure 4 shows the radial profile of the stress-optic constant for both fibers measured before and after annealing at 80°C. The evolution of the radial profile of $C(r)$ for Fiber 4 is comparable to our previous findings. The radial profile of $C(r)$ of Fiber 5, however, is not affected by the

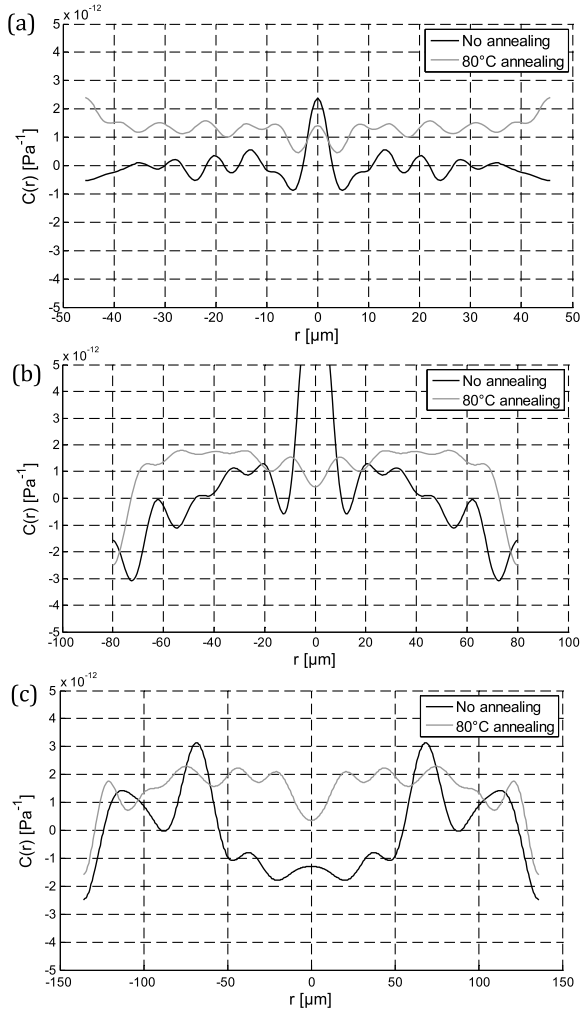

Fig. 2. Comparison of the radial distribution of the photoelastic coefficient $C(r)$ of the POFs under test without annealing and with 8 h annealing at 80°C in (a) Fiber 1, (b) Fiber 2, and (c) Fiber 3.

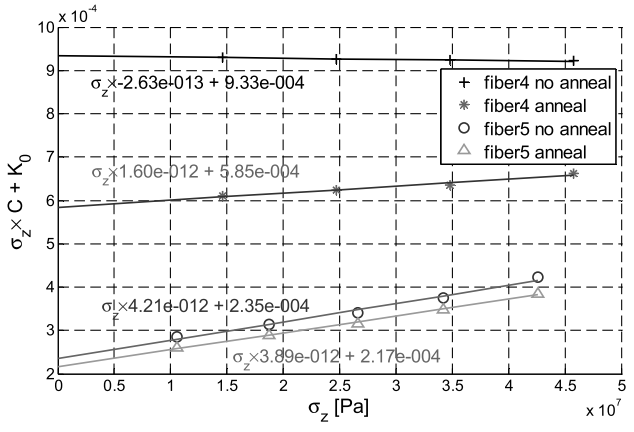

Fig. 3. $\sigma_z \times C + K_0$ as a function of the axial stress measured on samples of Fibers 4 and 5. The values of C and the extrapolated values of the residual stress are indicated in the graph along the respective linear fits.

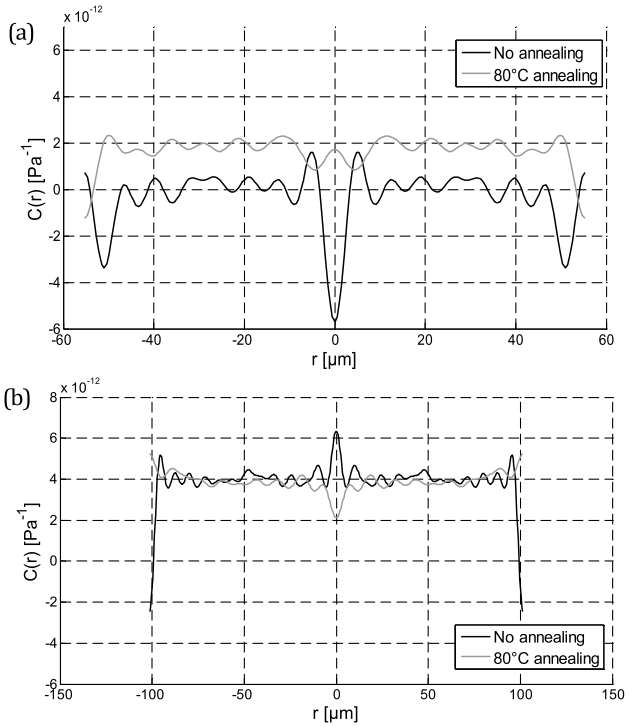

Fig. 4. Comparison of the radial distribution of the photoelastic coefficient $C(r)$ of (a) Fiber 4 and (b) Fiber 5 before and after 8 h annealing at 80°C.

annealing process. Recall that the preform of this fiber has been annealed for two weeks at 80°C. Note also that for Fiber 5, we find a value of C of 4×10^{-12} Pa^{-1}, which is larger than the values measured for Fibers 1 to 4.

To conclude, we have determined the radial profile of the photoelastic constant $C(r)$ and its mean value in five different polymer optical fibers. We have also analyzed the effect of annealing on that material parameter, and we quantified the impact of annealing on the residual stress in the POF. Annealing at 40°C and 60°C did not significantly affect $C(r)$ and K_0 for any of the fiber samples. Annealing at a higher temperature, i.e., 80°C, of fibers drawn from a preform without any specific annealing treatment did impact both parameters. The radial profile of $C(r)$ is more regular and clean, which may indicate a reduced variation of the material parameter C throughout the fiber section and an increased homogeneity in the cross section of the POF. Additionally, annealing increases significantly the mean value of $C(r)$, but decreases the residual birefringence throughout the fiber section. This may explain the findings reported in [14] i.e., the higher sensitivity to stress and strain, but a lower cross-sensitivity to strain and temperature of the annealed fiber.

The effect of annealing on a POF of which the preform has been annealed prior to drawing is different. This fiber is much less sensitive to thermal treatment, as shown with Fiber 5.

In future work, we will address the actual influence of annealing on the strain sensitivity of the fiber.

Funding. IWT-SBO Project (120024 "Self Sensing Composites-SSC"); Research Foundation Flanders (FWO); Methusalem and Hercules Foundations; Belgian Science Policy Interuniversity Attraction Pole (P7/35); Marie Curie Intra European Fellowship included in the 7th Framework Program of the European Union (project PIEF-GA-2013-628604); FCT Fellowship (SFRH/BPD/109458/2015).

REFERENCES

1. K. Peeters, Smart Mater. Struct. **20**, 013002 (2011).
2. N. G. Harbach, "Fiber Bragg gratings in polymer optical fibers," Ph.D. thesis (Ecole Polytechnique Fédérale de Lausanne, 2008).
3. F. Berghmans and H. Thienpont, *Optical Fiber Communication Conference (OFC)* (2014), pp. 3–5.
4. D. J. Webb, Meas. Sci. Technol. **26**, 092004 (2015).
5. A. Tagaya, T. Harade, K. Koike, and Y. Koike, J. Appl. Polym. Sci. **106**, 4219 (2007).
6. A. Tagaya, L. Lou, Y. Ide, Y. Koike, and Y. Okamoto, Sci. China Chem. **55**, 850 (2012).
7. R. M. Waxler, D. Horowitz, and A. Feldman, Appl. Opt. **18**, 101 (1979).
8. H. Ohkita, K. Ishibashi, D. Tsurumoto, A. Tagaya, and Y. Koike, Appl. Phys. A **81**, 617 (2005).
9. F. Ay, A. Kocabas, C. Kocabas, A. Aydinli, and S. Agan, J. Appl. Phys. **96**, 7147 (2004).
10. W. Primak, J. Appl. Phys. **30**, 779 (1959).
11. N. Lagakos and R. Mohr, Appl. Opt. **20**, 2309 (1981).
12. A. Bertholds and B. Dändliker, J. Lightwave Technol. **6**, 17 (1988).
13. W. Yuan, A. Stefani, M. Bache, T. Jacobsen, B. Rose, N. Herholdt-Rasmussen, F. K. Nielsen, S. Andresen, O. B. Sørensen, K. S. Hansen, and O. Bang, Opt. Commun. **284**, 176 (2011).
14. R. Oliveira, C. A. F. Marques, L. Bilro, and R. N. Nogueira, *23rd International Conference on Optical Fibre Sensors* (2014), Vol. **9157**, p. 9.
15. S. Acheroy, P. Merken, H. Ottevaere, T. Geernaert, H. Thienpont, and F. Berghmans, Appl. Opt. **52**, 8451 (2013).
16. S. Acheroy, P. Merken, T. Geernaert, H. Ottevaere, H. Thienpont, and F. Berghmans, Opt. Express **23**, 18943 (2015).
17. S. Acheroy, M. Patrick, G. Thomas, H. Ottevaere, H. Thienpont, and F. Berghmans, Proc. SPIE **9141**, 914115 (2014).
18. P. L. Chu and T. Whitbread, Appl. Opt. **21**, 4241 (1982).
19. H. Y. Liu, G. D. Peng, and P. L. Chu, IEEE Photon. Technol. Lett. **14**, 935 (2002).
20. Y. Luo, B. Yan, M. Li, X. Zhang, W. Wu, Q. Zhang, and G.-D. Peng, Opt. Fiber Technol. **17**, 201 (2011).
21. W. Wu, Y. Luo, X. Cheng, X. Tian, W. Qiu, B. Zhu, G. Peng, and Q. Zhang, J. Optoelectron. Adv. Mater. **12**, 1652 (2010).
22. H. Y. Liu, G. D. Peng, and P. L. Chu, IEEE Photon. Technol. Lett. **13**, 824 (2001).
23. G. Woyessa, A. Fasano, A. Stefani, C. Markos, K. Nielsen, H. K. Rasmussen, and O. Bang, Opt. Express **24**, 1253 (2016).
24. G. Woyessa, K. Nielsen, A. Stefani, C. Markos, and O. Bang, Opt. Express **46**, 643 (2011).
25. P. Stajanca, O. Cetinkaya, M. Schukar, P. Mergo, D. J. Webb, and K. Krebber, Opt. Fiber Technol. **28**, 11 (2016).
26. http://www.paradigmoptics.com/.
27. C. A. F. Marques, L. B. Birlo, N. J. Alberto, D. J. Webb, and R. N. Nogueira, Opt. Commun. **307**, 57 (2013).